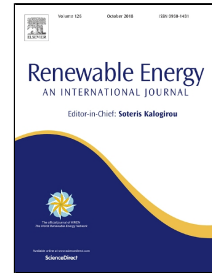


# Accepted Manuscript

Effects of injection strategies on combustion and emission characteristics of a common-rail diesel engine fueled with isopropanol-butanol-ethanol and diesel blends



Gang Li, Timothy H. Lee, Zhien Liu, Chiafon F. Lee, Chunhua Zhang

PII: S0960-1481(18)30751-1  
DOI: 10.1016/j.renene.2018.06.099  
Reference: RENE 10255  
To appear in: *Renewable Energy*  
Received Date: 13 March 2018  
Accepted Date: 25 June 2018

Please cite this article as: Gang Li, Timothy H. Lee, Zhien Liu, Chiafon F. Lee, Chunhua Zhang, Effects of injection strategies on combustion and emission characteristics of a common-rail diesel engine fueled with isopropanol-butanol-ethanol and diesel blends, *Renewable Energy* (2018), doi: 10.1016/j.renene.2018.06.099

This is a PDF file of an unedited manuscript that has been accepted for publication. As a service to our customers we are providing this early version of the manuscript. The manuscript will undergo copyediting, typesetting, and review of the resulting proof before it is published in its final form. Please note that during the production process errors may be discovered which could affect the content, and all legal disclaimers that apply to the journal pertain.

1 **Effects of injection strategies on combustion and emission characteristics of a common-rail**  
2 **diesel engine fueled with isopropanol-butanol-ethanol and diesel blends**

3 Gang Li<sup>a,b</sup>, Timothy H. Lee<sup>b</sup>, Zhien Liu<sup>c</sup>, Chiafon F. Lee<sup>b,\*</sup>, Chunhua Zhang<sup>a</sup>

4 <sup>a</sup>School of Automobile, Chang'an University, Xi'an 710064, PR China;

5 <sup>b</sup>Department of Mechanical Science and Engineering, University of Illinois at Urbana  
6 Champaign, IL 61801, USA;

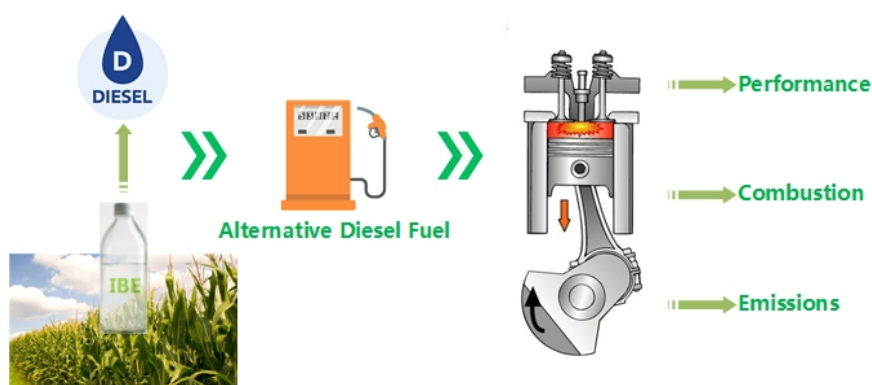
7 <sup>c</sup>Hubei Key Laboratory of Advanced Technology for Automotive Components, Wuhan  
8 University of Technology, Wuhan, China, 430070.

9 \*Corresponding author: Chiafon F. Lee, E-mail: cflee@illinois.edu

10 **Abstract:** This study is aimed to investigate the performance, combustion, and emissions of a  
11 common-rail diesel engine fueled with IBE and diesel blends. Two blends of IBE and diesel fuel,  
12 denoted as IBE15 (15% IBE and 85% diesel in volume) and IBE30 (30% IBE and 70% diesel in  
13 volume), were tested under different injection strategies. The experimental results show that  
14 compared with single injection, the in-cylinder pressure and heat release rate curves (*HRR*) for all  
15 the tested fuels under double injection cases are less severe. That is to say, a pilot injection can  
16 reduce knocking combustion and ringing intensity when blending a high ratio of IBE into diesel.  
17 Furthermore, double injection is helpful in improving both engine performance and economy for  
18 all the tested fuels, especially for IBE30. For almost all the tested conditions, both IBE15 and  
19 IBE30 present a potential to reduce soot emissions but increase NO<sub>x</sub> emissions. A pilot injection  
20 is favorable to reduce NO<sub>x</sub> emissions but causes the soot emissions to increase. Results also show  
21 that the flame lift-off length of IBE30 is much longer than pure diesel. This feature may result in  
22 better air-fuel mixing, which then contributes to reduce soot emissions.

23 **Keywords:** isopropanol-butanol-ethanol (IBE), IBE/diesel blends, injection strategy, combustion,  
 24 emissions

25 **Graphical abstract:**



26

## 27 1. Introduction

28 Alternative fuels, such as ethanol, dimethyl ether, natural gas, bio-diesel, and butanol, are a  
 29 good choice for conventional internal combustion engines to reduce the transportation fuel usage  
 30 and to meet the stringent exhaust emission regulations [1-3]. Among those fuels, butanol has been  
 31 considered as a promising replacement for diesel because of its good miscibility, high energy  
 32 density and cetane number, low auto-ignition temperature, and evaporation pressure [4,5]. It has  
 33 already been proven that after blending butanol into diesel, soot emissions of diesel engines could  
 34 be drastically reduced [6,7]. Furthermore, high-ratio butanol and diesel blends coupled with EGR  
 35 is capable of simultaneously reducing soot and NO<sub>x</sub> emissions [8]. In general, butanol is  
 36 fermented from lignocellulosic (e.g., wheat straw, bagasse, switchgrass, corn straw, and barley  
 37 straw, etc.) and non-cellulosic (e.g., sugarcane, glucose, sago, and corn, etc.) feedstock using  
 38 *Clostridium beijerinckii* or *Clostridium acetobutylicum* [9-11]. Additionally, the lignocellulosic  
 39 materials have been considered as the more abundant and cheaper feedstock for the fermentation  
 40 process of butanol [12]. The intermediate fermentation product of butanol is acetone, n-butanol,

41 and ethanol mixture (ABE) at a volume ratio of roughly 3:6:1. This ABE mixture undergoes a  
42 difficult separation and purification process to obtain pure butanol. Although butanol shows a  
43 great potential in diesel engines, the high separation cost and low production efficiency make it  
44 currently less competitive in comparison with diesel, gasoline, and ethanol.

45 In recent years, numerous researchers begun to directly use ABE as an alternative fuel in  
46 engines to utilize the numerous advantages of butanol and to avoid the aforementioned separation  
47 cost during butanol fermentation. Li et al. [13] investigated the water-containing ABE and  
48 gasoline blends in a spark ignition engine. They found that the addition of water-containing ABE  
49 in gasoline could improve the engine performance and reduce the CO and HC emissions.  
50 Nithyanandan et al. [14] compared the performance and emissions of different ABE fuels in a  
51 spark ignition engine. They reported that high-acetone ABE was more suited for use as an  
52 alternative fuel than low-acetone ABE when considering the thermal efficiency. Lee et al. [15]  
53 experimentally studied the combustion characteristics of ABE and diesel blends in a diesel  
54 engine. The results have shown that the indicated thermal efficiency increased with even a small  
55 ratio of ABE blended into diesel. Lin et al. [16] also investigated the combustion process of ABE  
56 in a diesel engine. They pointed out that the combustion process of ABE-containing fuels was  
57 premixed-dominant combustion. Additionally, there were some studies focused on the spray  
58 combustion characteristics and soot emission of ABE and diesel blends. Wu et al. [17,18]  
59 conducted various experiments in a constant volume chamber to investigate the spray combustion  
60 characteristics of the ABE blended with diesel. They found that ABE blended into diesel with a  
61 50% ratio by volume could maintain diesel combustion characteristics but result in a lower  
62 natural flame luminosity and shorter combustion duration. Wu et al. [19] also conducted some

63 experiments to study the soot formation of ABE and diesel blends. Their results showed that the  
64 soot cloud region and intensity reduced when ABE blended into diesel. Zhou et al. [20] also  
65 arranged various experiments to study the spray and soot emission characteristics of ABE and  
66 diesel blends in a constant volume chamber. They pointed that soot emissions of ABE and diesel  
67 blends could be further reduced by adopting low-temperature combustion. In order to study  
68 puffing and micro-explosions of ABE and diesel blends, Ma et al. [21, 22] conducted various  
69 experiments on the droplet evaporation through the droplet suspension technique. They reported  
70 that strong puffing was observed during the ABE–diesel blends evaporation process at 823 K but  
71 currently no micro-explosion phenomenon was captured in their test conditions.

72 Even though ABE has numerous advantages when utilized in internal combustion (IC)  
73 engines, the poor properties of acetone in ABE restrict its further development. First, the acetone  
74 in ABE is corrosive to rubber engine parts [23-24]. Furthermore, the acetone in ABE has a very  
75 low flash boiling point, which makes ABE hard to transport and store in traditional implements  
76 [25]. In this respect, various metabolic engineering strategies have been employed to convert  
77 acetone into isopropanol, which seems to have more favorable physicochemical properties in  
78 comparison to acetone including higher viscosity, higher energy density, and higher flash point.  
79 Some gene-edited bacterial strains such as *Clostridium acetobutylicum* ATCC824 [26],  
80 *Clostridium acetobutylicum* DSM792-ADH [27] and *Clostridium acetobutylicum* BKM19 [28],  
81 that capable of substantially converting acetone into isopropanol were developed. The new  
82 biofuel consisting of isopropanol, butanol and ethanol (IBE) has already been studied by some  
83 researchers in internal combustion engines. Li et al. [29,30] experimentally studied the  
84 combustion and emissions of IBE and gasoline blends in a spark ignition engine. They indicated

85 that the addition of IBE into gasoline could improve the engine thermal efficiency and reduce  
86 pollutant emissions. Lee et al. [31] has investigated the combustion and emission characteristics  
87 of the IBE in a diesel engine and found that with the addition of IBE lead to a reduction in soot  
88 emission. It also has been proved by Li et al. [32] that NO<sub>x</sub> and soot emissions can be reduced  
89 simultaneously by using high-ratio IBE under EGR conditions. Unfortunately, the previously  
90 studies only blended IBE in diesel with a relatively low ratio and tested the IBE in some  
91 conventional engine operation conditions. In this respect, it is necessary to further study the  
92 combustion and emission characteristics of the diesel engine fueled with IBE and diesel blends.

93 In this study, the authors conducted a detailed experimental study on a single-cylinder and  
94 common-rail diesel engine fueled with IBE and diesel blends to evaluate the potential of IBE as  
95 an alternative fuel. Two blends of butanol and diesel fuel, denoted as IBE15 (15% IBE and 85%  
96 diesel in volume) and IBE30 (30% IBE and 70% diesel in volume), were tested. Moreover,  
97 experiments are performed to investigate how the injection strategy influences the performance,  
98 combustion, and emissions of the diesel engine fueled with different fuels. The IBE mixture used  
99 in this study was mixed by analytical surrogate fuels with volumetric ratios of 3:6:1 to simulate  
100 the fuel mixtures from the fermentation process of butanol.

## 101 **2. Test apparatus and procedure**

### 102 *2.1. Experimental setup*

103 The experiments were conducted on a direct injection, single cylinder and common-rail  
104 diesel engine (AVL 5402) manufactured by the AVL company in Austria. The specifications of  
105 the test engine are presented in [Table 1](#). An eddy current dynamometer (GE TCL-15, 4-35-1700)  
106 with a rated power up to 26.1 kW was connected to the test engine. This dynamometer has a

107 three-phase asynchronous motor, which can both absorb and supply torque. The engine torque  
 108 and speed were controlled by the Dyne system controller (DYN-LOC IV).

109 **Table 1.** The specifications of the diesel engine.

Items	Specifications
Model	AVL 5402
Type	1-cylinder, direct injection
Fuel injection system	BOSCH CP3 common rail
Bore (mm)× stroke (mm)	85 × 90
Displacement (L)	0.51
Compression ratio	17.5:1
Number of valves	4
Rated power (kw @ rpm)	6 @ 4200
Number of injection holes	5
Diameter of injection holes (mm)	0.18

110 **Fig. 1** shows the schematic of the experimental apparatus used in this study. The fuel  
 111 injection system of the test engine was an advanced common-rail system, which is capable of  
 112 four injections per cycle and a rail pressure up to 100 MPa. This common-rail system is coupled  
 113 with an open-loop prototype ETAS engine control unit designed by AVL. The injection  
 114 parameters such as injection quantity, injection pressure, and injection timing could be controlled  
 115 using the INCA software. Two fuel pumps (a high-pressure pump and a low-pressure pump) were  
 116 used in the fuel supply system to provide a stable supply of fuel from fuel tank to the common-  
 117 rail.

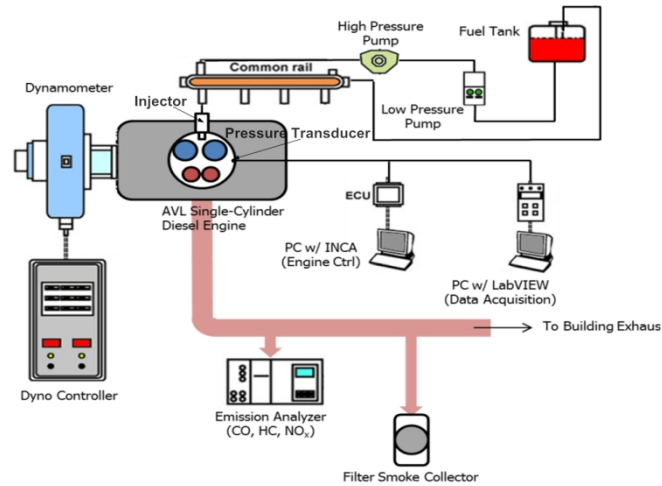


**Fig.1.** Schematic of experimental apparatus.

118

119

120 Air-fuel ratios and NO<sub>x</sub> emissions were measured using a Horiba MEXA-270 analyzer. HC  
 121 and CO emissions were measured using a Horiba MEXA-554JU analyzer. Soot emissions were  
 122 obtained using a standard filter paper method, which will be described at the later section. The in-  
 123 cylinder pressure signal was measured with a piezoelectric pressure transducer (6152B, Kistler)  
 124 coupled with a charge amplifier (3057-AO1, AVL). Moreover, a crank angle encoder (BEI  
 125 XH25D) with a resolution of 0.1° crank angle (CA) was mounted at the end of the crankshaft to  
 126 record the crank angle position. In each test condition, the in-cylinder pressure data was collected  
 127 over 150 continuous cycles with a crank angle (CA) sampling interval of 0.25 °CA by a  
 128 LabVIEW acquisition system, which consists of a NI SCXI-1000 board, a NI PCI-MIO-16E4  
 129 board and a self-made LabVIEW code. The in-cylinder pressure data were averaged to eliminate  
 130 the effect of cycle-to-cycle variations. The various combustion parameters such as heat release  
 131 rate (*HRR*) and combustion phasing were calculated from the averaged pressure trace. The  
 132 measuring accuracy of each instrument is given in [Table 2](#).

133

**Table 2.** Accuracy of measured parameters.

Equipment	Measured parameters	Range	Accuracy
-----------	---------------------	-------	----------

Eddy current dynamometer	Speed	1-5000 rpm	0.2%
	Torque	0-300 N m	0.5%
Horiba MEXA-554JU analyzer	CO emission	0-10 vol.%	0.06%
	HC emission	0-10000 ppm	1 ppm
Horiba MEXA-270 analyzer	NOx emission	0-3000 ppm	3%

## 134 2.2. Experimental procedure

135 Two blends of butanol and diesel fuel, denoted as IBE15 and IBE30, were tested in this  
 136 study. Detailed experiments were carried out at different injection strategies at the engine load of  
 137 0.54 MPa (brake mean effective pressure, BMEP) and an engine speed of 1500 r/min. To  
 138 investigate the effects of the single injection, the engine was operated only with a main injection  
 139 with its timing varied from 6 °CA to 18 °CA BTDC in steps of 3 °CA. To investigate the effects  
 140 of double injection, the engine was operated with the main injection coupled with a pilot  
 141 injection. In this stage, the pilot injection timing (PIT) was swept from 25 °CA to 45 °CA BTDC  
 142 in steps of 5 °CA, but the main injection timing (MIT) was fixed at 9 °CA BTDC. The detailed  
 143 test conditions are presented in [Table 3](#). At the beginning of the test, the engine was warmed-up  
 144 until the coolant and lubricating oil temperature reached about 85°C. Then the engine was  
 145 adjusted to the test conditions using the INCA software. After the engine had reached steady-  
 146 state, the in-cylinder pressure and exhaust emissions were recorded. Each test condition was  
 147 repeated more than three times to reduce the experimental uncertainties and to ensure that the  
 148 results were repeatable.

149 **Table 3.** Test conditions.

Items	MIT Cases	PIT Cases
-------	-----------	-----------

Fuels	Diesel, IBE15, IBE30	
Engine speed (rpm)	1500	
Engine load (MPa)	0.54	
Pilot injection timing (°CA BTDC)	None	25,30,40,45
Main injection timing (°CA BTDC)	6,9,12,15,18	9
Injection pressure (MPa)	60	

### 150 2.3. Test fuels

151 Commercial diesel with a sulfur content lower than 50 ppm was selected as baseline fuel in  
 152 this study. The IBE mixture was prepared with analytical grade surrogate fuel, namely  
 153 isopropanol (99.5%), n-butanol (99.5%) and ethanol (99.8%). A temperature-controlled magnetic  
 154 stirrer was used to mix the IBE mixture to a volumetric ratio of 3:6:1 (A:B:E). This ratio was to  
 155 simulate the composition of the fuel mixtures from the fermentation process of bio-butanol. The  
 156 detailed physicochemical properties of the test fuels are listed in Table 4. It should be noted that  
 157 the cetane number of the individual fuels in Table 4 was taken from reference [33]. The  
 158 properties of the IBE mixture were calculated according to simple mixing rules in [34].  
 159 Afterwards, the IBE mixture were mixed with diesel to prepare the fuel blends. The fuel blends  
 160 used in this study were denoted as IBE15 and IBE30, which means the volumetric ratios of the  
 161 IBE mixture in the fuel blends were 15% and 30%, respectively.

162 **Table 4.** Fuel properties.

Parameters	Individual fuels				Fuel blends
	Diesel	ethanol	Isopropanol	n-Butanol	IBE
Chemical formula	C <sub>10</sub> -C <sub>22</sub>	C <sub>2</sub> H <sub>5</sub> OH	C <sub>3</sub> H <sub>7</sub> OH	C <sub>4</sub> H <sub>9</sub> OH	-

Cetane number	52.65	8	12	15.92	13.952
Octane number	-	100	112	87	95.8
Oxygen content (wt.%)	-	34.8	26.6	21.6	24.4
Density (kg/m <sup>3</sup> )	820-860	795	786	813	803.1
Lower heating value (MJ/kg)	42.7	26.8	30.4	33.1	31.7
Boiling temperature (°C)	282-338	78	84	118	-
Latent heat (kJ/kg)	260	904	758	582	667
Stoichiometric AFR	14.3	9.0	10.4	11.2	10.7
Auto-ignition temperature	250	420	399	343	-

## 163 2.4. Data processing

### 164 2.4.1. Brake Specific Fuel Consumption

165 Since IBE and diesel have different lower heating values, the equivalent heat brake specific  
 166 fuel consumption (BSFC) was used in this study to indicate the thermal efficiency. The  
 167 equivalent BSFC could be calculated as follows.

$$168 \text{ BSFC} = B_e \times \frac{H_D \times \rho_D \times V_D + H_{IBE} \times \rho_{IBE} \times V_{IBE}}{H_D \times (\rho_D \times V_D + \rho_{IBE} \times V_{IBE})} \quad (1)$$

169 where, BSFC represents the equivalent BSFC of each fuel, namely pure diesel, IBE15 or IBE30.  
 170  $B_e$  represents the actual BSFC of each fuel.  $V_D(V_{IBE})$  represents the volumetric fraction of diesel  
 171 (or IBE).  $\rho_D(\rho_{IBE})$  represents the density of diesel (or IBE).  $H_D(H_{IBE})$  represents the lower heating  
 172 value of diesel (or IBE). It should be noted that the lower heating value of IBE used in this study  
 173 was calculated according to the simple mixing rules described in reference [34].

### 174 2.4.2. Soot Emissions

175 Soot emissions were measured using a standard filter paper method. Raw exhaust gases were  
 176 drawn through a 7/8" round filter paper using a vacuum pump. Rectangular strips of filter paper

177 supplied by Grainger Industrial Supply (#6T167) were cut into discs and placed in a filter holder  
 178 taken from a Bacharach True-Spot smoke meter. Condensed water and oil were removed by  
 179 installing a line filter after the vacuum pump. The filter paper blackening (PB) was measured  
 180 using a digital scanner after the samples were collected. The PB value could be considered as the  
 181 filter smoke number (FSN) as described in [14,15], given by

$$182 \quad PB = \left( 100 - \frac{R_p}{R_f} \times 100\% \right) / 10 \quad (2)$$

183 where  $R_p$  and  $R_f$  are the reflectometer value of sample and unblackened paper, respectively.

#### 184 2.4.3. Combustion Phasing

185 The ignition delay is defined as the interval of crank angle between the start of injection and  
 186 the start of combustion (SOC). The combustion duration is defined as the interval of crank angle  
 187 between the start of combustion and the end of combustion (EOC) [35]. In this study, the start of  
 188 injection was recorded from the INCA software. The SOC and EOC were calculated according to  
 189 the first law of thermodynamics. Firstly, the net heat release rate was calculated as follows:

$$190 \quad \frac{dQ}{d\theta} = \frac{\gamma}{\gamma-1} V \frac{dV}{d\theta} + \frac{1}{\gamma-1} P \frac{dV}{d\theta} \quad (3)$$

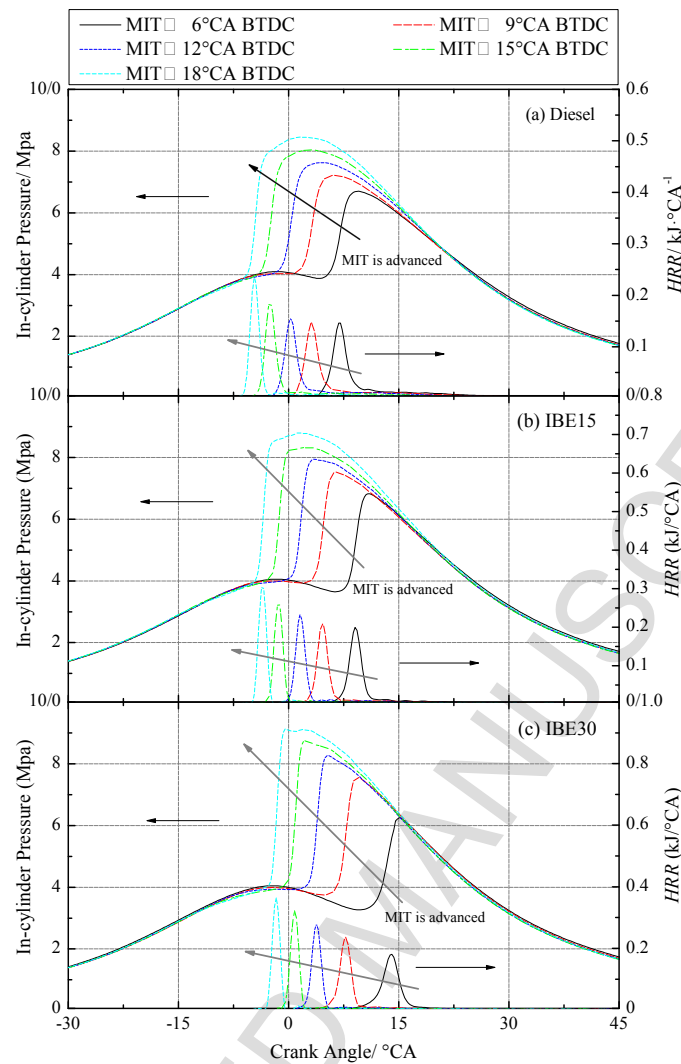
191 where  $\gamma$  is the ratio of specific heats,  $P$  and  $V$  are the in-cylinder pressure and volume at a crank  
 192 angle, respectively. Then the cumulative heat release from the air-fuel mixture can be obtained by  
 193 integrating Eq. (3). Subsequently, the crank angle where 10% and 90% of the total heat released  
 194 can be found to define SOC and EOC, respectively [36]. The combustion center, which defined  
 195 as the crank angle where 50% of the total heat released, can be found in the same way.

### 196 3. Results and discussion

#### 197 3.1. Effects of single injection

## 198 3.1.1. Combustion characteristics

199 Fig. 2 shows the in-cylinder pressure and *HRR* for different fuels at various MITs. The  
200 results show that the MIT has remarkable influence on the combustion process of the tested fuels.  
201 When the MIT is advanced, the peak in-cylinder pressure and *HRR* increase for all the test fuels  
202 significantly. The main reason is the temperature at the crank angle where the fuel injected ( $T_{inj}$ )  
203 [37]. When the MIT is gradually advanced,  $T_{inj}$  decreases. Thus, the fuel injected to the cylinder  
204 undergoes a long ignition delay, which can potentially increase the amount of homogeneous air-  
205 fuel mixture formed during the ignition delay and therefore enhance the premixed combustion.  
206 For all the tested fuels, the combustion processes advanced as the MIT is advanced. However, as  
207 seen from an equal MIT condition, the combustion processes of IBE15 and IBE30 are delayed in  
208 comparison to pure diesel, especially in the case of IBE30. This is mainly because the  
209 combustion processes of IBE15 and IBE30 are also greatly affected by the fuel properties of IBE,  
210 including the cetane number and latent heat. When IBE and diesel blends are injected into the  
211 cylinder, they need to absorb heat to vaporize and hence lower the in-cylinder temperature at the  
212 compression stroke. On the other hand, the two fuel blends are hard to ignite at low temperatures  
213 due to their poor ignitability and low activation energy. All those factors contribute to prolonging  
214 the ignition delay and retarding the combustion process. It also can be seen that almost in all test  
215 cases, the peak values of the in-cylinder pressure and *HRR* for the two fuel blends are much  
216 higher than that of pure diesel because of the enhanced premixed combustion when IBE is  
217 blended in diesel. Nevertheless, at the MIT of 6 °CA BTDC, the pressure curve for the IBE30  
218 exhibits a lowest peak in comparison to pure diesel and IBE15 due to the over retarded  
219 combustion process.



220

221

**Fig. 2.** In-cylinder pressure and  $HRR$  for different fuels with various MITs.

222

223

224

225

226

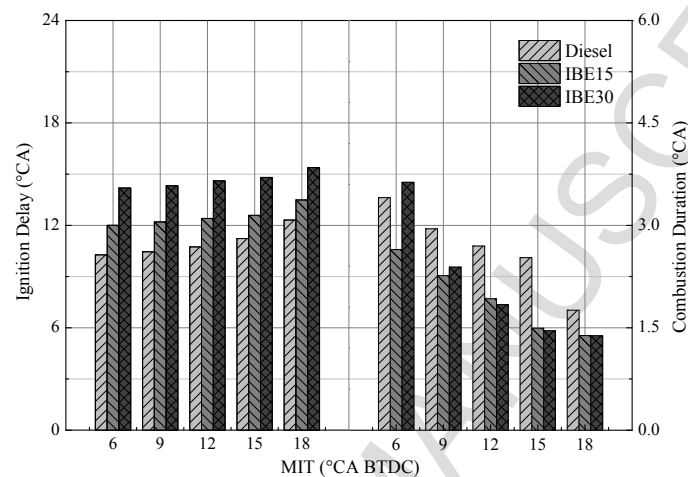
227

228

229

**Fig. 3** displays the changes of the ignition delay and combustion duration of different fuels with various MITs. It can be seen that for all test fuels, the ignition delay increases as the MIT is advanced. Additionally, the blend of IBE in diesel has further prolonged the ignition delay for the same reason discussed in the above section. For the combustion duration, it noticeably shortened when the MIT is advanced. This is mainly because at an early MIT, an abundant amount of homogeneous air-fuel mixture is formed during the ignition delay and afterwards burns at a rapid speed. In most test conditions, the combustion duration for the two fuel blends is shorter than that of pure diesel. One reason is that the OH radicals produced by IBE improves the combustion

230 speed. Another reason is that the long ignition delay from the IBE-diesel blend enhances the  
 231 premixed combustion. However, at 6 °CA BTDC, IBE30 has the longest combustion duration in  
 232 comparison to diesel and IBE15. This is because at 6 °CA BTDC, the combustion phasing of  
 233 IBE30 has been overly retarded, which noticeably slows down the combustion speed of air-fuel  
 234 mixture and causes the combustion of IBE30 to deteriorate.

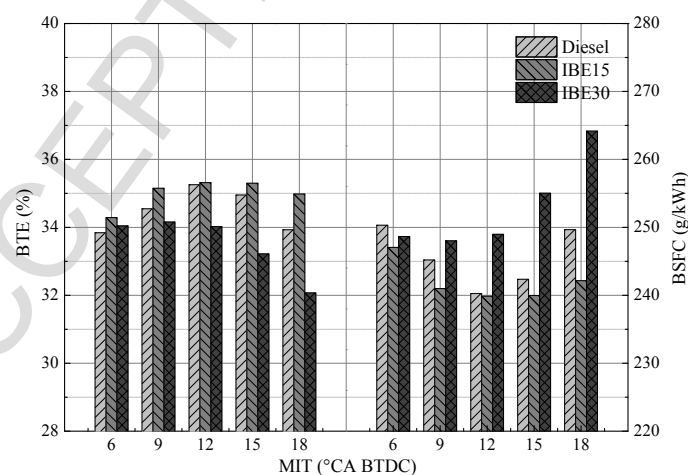


235  
 236 **Fig. 3.** Ignition delay and combustion duration for different fuels with various MITs.

### 237 3.1.2. Engine performance

238 The effects of MIT on the BTE and BSFC of different fuels have been illustrated in Fig. 4.  
 239 The BTE indicates how well an engine can convert the chemical energy in a fuel into mechanical  
 240 energy. It can be seen that for all the tested fuels, BTE first increases and then decreases when the  
 241 MIT is advanced. At the beginning, the combustion process is gradually swept to TDC when the  
 242 MIT is advanced, which causes the BTE to increase. Then when the MIT is further advanced,  
 243 BTE reduces because the combustion process is swept to the compression stroke and separated  
 244 from TDC. Compared with pure diesel and IBE30, the BTE of IBE15 is always higher due to the  
 245 reduced combustion duration and increased extent of constant volume combustion. Although the  
 246 premixed combustion of IBE30 is stronger than that of pure diesel and IBE15, the BTE of IBE30

247 is the lowest almost in all the test conditions. At small MIT, the low BTE of IBE30 is caused by  
 248 the retarded combustion process, but at large MITs, it is caused by the increased negative work. It  
 249 also can be seen that BSFC shows an opposite trend with BTE. When the MIT is advanced, it  
 250 first decreases and then increases for all the tested fuels. Almost in all the test conditions, the  
 251 BSFC for IBE15 is lower, but for IBE30 it is higher in comparison to pure diesel. First, the  
 252 premixed combustion is enhanced when IBE is blended in diesel and thus contributes to a  
 253 reduction in BSFC. Second, more fuel is needed for maintaining the engine runs at the same load  
 254 since the energy density is reduced when a large amount of fuel IBE is blended in diesel. In the  
 255 competition of all these mechanisms, the previous mechanism plays the dominate role for IBE15  
 256 and the last mechanism plays the dominate role for IBE30. The optimal engine performance and  
 257 economy for the pure diesel and IBE15 is found at 12 °CA BTDC but for IBE30 is found at 9  
 258 °CA BTDC. The main reason is that IBE30 has the strongest premixed combustion among the  
 259 tested fuels, thereby it can weaken the negative effect of retarded MIT and combustion phasing.  
 260 This result means that IBE30 is more tolerant to retard MIT than pure diesel and IBE15.



261  
262 **Fig. 4.** BTE and BSFC for different fuels with various MITs.

263 *3.1.3. Emission characteristics*

264 The variation of the CO and HC emissions with different MITs for the different fuels are  
265 given in Fig. 5. It can be clearly seen that for all of the tested fuels, the CO and HC emissions  
266 reduce when the MIT is advanced from 6 to 15 °CA BTDC. This is mainly because the advanced  
267 MIT results in longer ignition delay and higher combustion efficiency, and hence reduce the fuel  
268 consumption and incomplete combustion. However, when the MIT is further advanced, the CO  
269 and HC emissions for all of the tested fuels increase. The main reason is that as the MIT is further  
270 advanced, the whole combustion process is swept towards the compression stroke, which causes  
271 the negative work to increase significantly. In this stage, more fuel is needed to maintain the  
272 engine runs at an identical load and then the air-fuel mixture undergoes a rich combustion. Also,  
273 it can be seen that almost in all of the test conditions, the CO and HC emissions of the IBE15 and  
274 IBE30 are higher than that of diesel emissions. This can be explained by the following reasons.  
275 First, the poor ignitability and high cooling effect of IBE causes the in-complete combustion to  
276 increase. Second, some unburned IBE-air mixtures are exhausted into emissions directly during  
277 the scavenging process. Third, the quenching effect at the chamber crevice and cylinder wall,  
278 which may cause HC emissions to increase, is strengthened when the IBE mixture is blended into  
279 diesel. At the MIT of 18, the CO and HC emissions of IBE15 and IBE30 are lower than that of  
280 pure diesel. This is mainly because the oxygen content and OH radicals produced by IBE  
281 suppresses the increase of CO and HC emissions at the over advanced MIT.

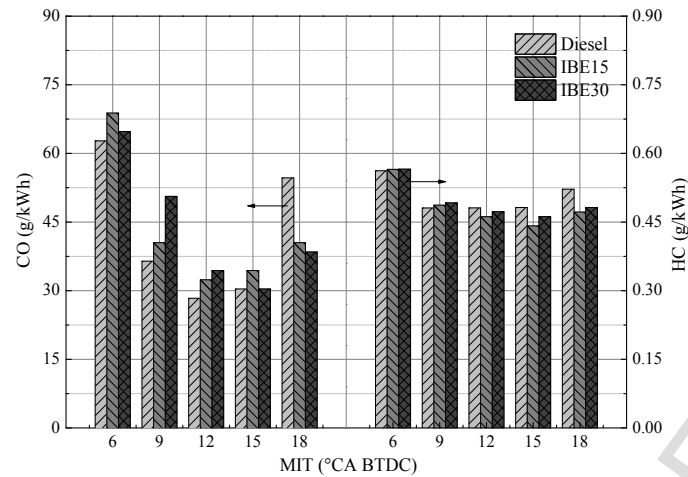


**Fig. 5.** CO and HC emissions for different fuels with various MITs.

282

283

284

285

286

287

288

289

290

291

292

293

294

295

296

297

298

The changes of NO<sub>x</sub> and soot emissions along with MITs for different fuels are presented in

[Fig. 6](#). It is observed that NO<sub>x</sub> emissions of all the tested fuels decrease notably as the MIT is

advanced due to the enhanced premixed combustion. Furthermore, NO<sub>x</sub> emissions for the two

fuel blends are higher than that of pure diesel since the premixed combustion is further enhanced

and oxygen content is increased when IBE is blended in diesel. For the soot emissions, it first

decreases as the MIT is advanced from 6 to 15 °CA BTDC but then increases as the MIT is

advanced to 18 °CA BTDC. This is because at the MIT of 18 °CA BTDC, the increased negative

work and deteriorated combustion efficiency makes the fuel consumption increase and the air-

fuel mixture to become rich. In addition, it is observed that the soot emissions of IBE15 and

IBE30 are always lower than that of pure diesel. The detailed mechanisms are shown as follows.

First, the smoke precursors can be effectively oxidized by the OH radicals produced by IBE.

Second, the alcohol fuel has a higher chance to prevent the formation of polycyclic aromatic

hydrocarbons, which is the main ingredient of soot precursors [38-39]. Finally, the premixed

combustion is enhanced and the diffusion combustion is weakened when the IBE is blended into

diesel, and thus may have the potential to further reduce soot emissions.

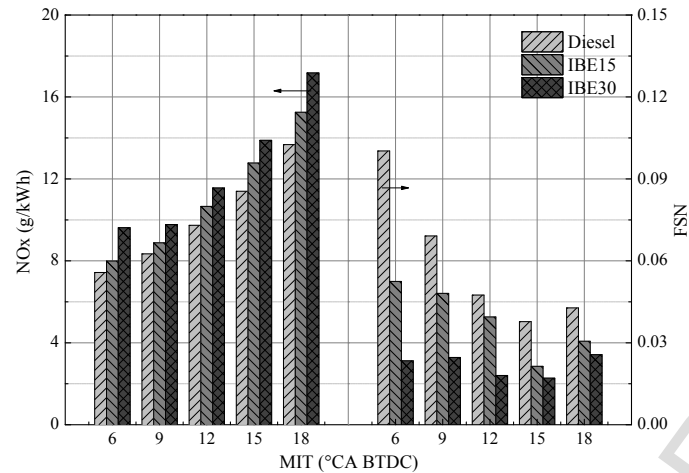


**Fig. 6.** NOx and soot emissions for different fuels with various MITs.

299

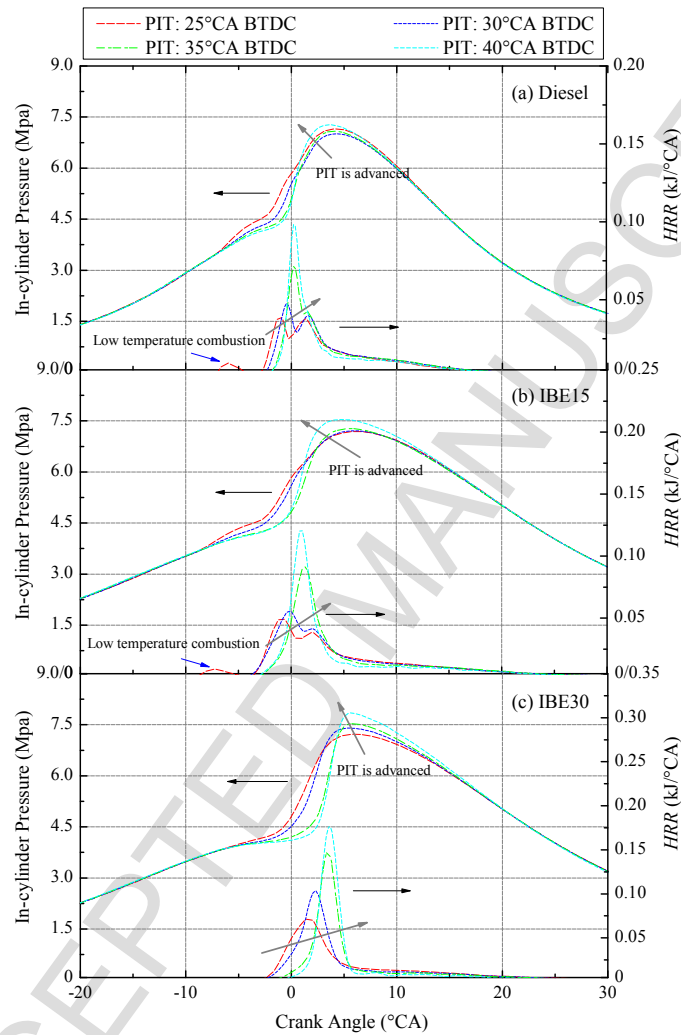
300

### 301 3.2. Effects of double injection

#### 302 3.2.1 Combustion characteristics

303 **Fig. 7** shows the in-cylinder pressure and *HRR* for different fuels at various PITs. The results  
 304 show that with a pilot injection, the pressure and *HRR* curve for all the tested fuels become less  
 305 severe and their peak values are noticeably lower in comparison to the single-injection  
 306 conditions. This is because the homogeneous air-fuel mixture and activated energy prepared by  
 307 the pilot injected fuels shorten the ignition delay and weaken the premixed combustion [40]. The  
 308 gentle pressure and *HRR* curve lead to the reduction in engine noise and ringing intensity. In most  
 309 test conditions, the peak in-cylinder pressure and *HRR* noticeably increase as the PIT is advanced.  
 310 The main reason is that more homogeneous air-fuel mixture formed during the ignition delay at  
 311 large PIT, which afterwards leads to a strong premixed combustion. The *HRR* curve for diesel  
 312 and IBE15 presents a double or triple peak profile at a small PIT while a single peak profile at  
 313 large PIT. However, for IBE30, its *HRR* curve always presents a single peak profile due to  
 314 prolonged ignition delay and enhanced premixed combustion. For diesel and IBE30, low  
 315 temperature combustion can be seen from the *HRR* curve at the PIT of 25 °CA BTDC.

316 Nevertheless, the same phenomenon cannot be found at the *HRR* curve of IBE30 since its poor  
 317 ignitability. When the PIT is larger than 25 °CA BTDC, the low temperature combustion  
 318 disappears for all the tested fuels since the pilot fuel is hard to auto-ignite at an even lower  
 319 temperature condition.

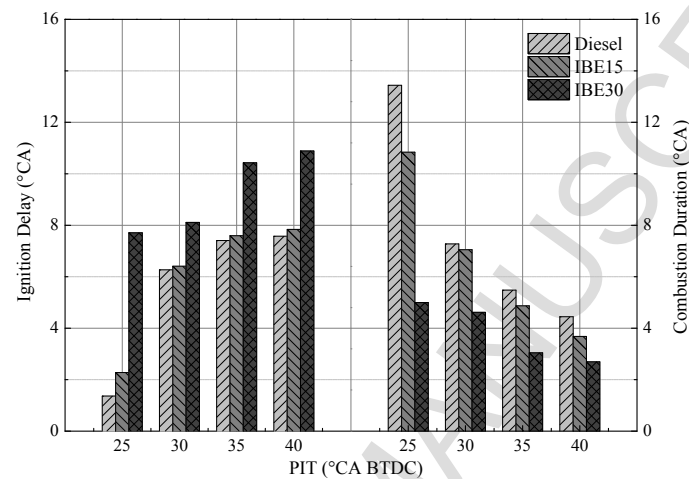


320

321 **Fig. 7.** In-cylinder pressure and *HRR* for different fuels with various PITs.

322 **Fig. 8** displays the changes of the ignition delay and combustion duration of different fuels  
 323 with various PITs. It can be observed that, with a pilot injection, the ignition delay is shortened  
 324 and the combustion duration is prolonged for all the tested fuels. At the PIT of 25 °CA BTDC,  
 325 the combustion duration of the diesel and IBE15 are almost three times longer than that of single  
 326 injection due to diffusion combustion. When the PIT is advanced, the ignition delay for all the

327 tested fuels is prolonged. This is attributed to the reduced temperature at the point where the pilot  
 328 fuel is injected. This prolonged ignition delay results in a stronger premixed combustion and a  
 329 shorter combustion duration as shown in Fig. 8. Compared with pure diesel, the two fuel blends  
 330 always show a longer ignition delay but shorter combustion duration in the tested conditions  
 331 because the fuel properties of IBE discussed before.

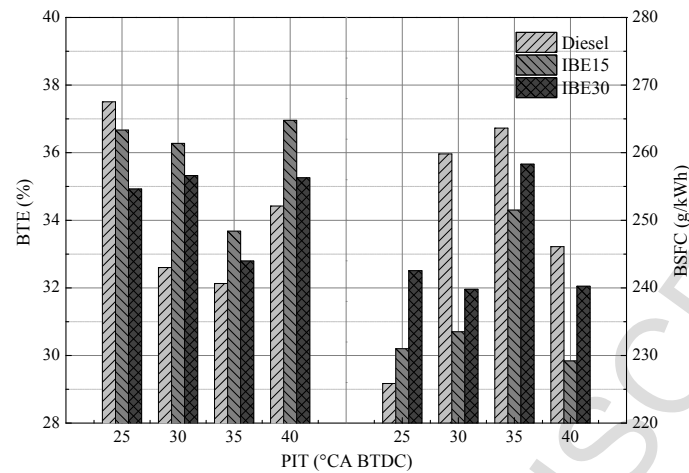


332  
 333 **Fig. 8.** Ignition delay and combustion duration for different fuels with various PITs.

### 334 3.2.2 Engine performance

335 The effects of PIT on the BTE and BSFC of different fuels are indicated in Fig. 9. The  
 336 results show that for almost at all the tested conditions the engine performance and fuel economy  
 337 for the tested fuels improved with a pilot injection because the pilot helped the main spray  
 338 develop and combust, unlike the results of single injection. IBE30 exhibits a better engine  
 339 performance and fuel economy than diesel at most tested conditions when the pilot injection is  
 340 adopted. This is mainly because the strong premixed combustion of IBE30 is further enhanced  
 341 and promoted by the pilot fuel. The results also show that when the PIT is advanced, both the  
 342 engine performance and fuel economy first deteriorate and then improve. This is because the  
 343 negative effect of the retarded combustion process is strengthened when the PIT is gradually

344 swept from 25 to 35 °CA BTDC, but then weakened by the significantly enhanced premixed  
 345 combustion at the PIT of 40 °CA BTDC.

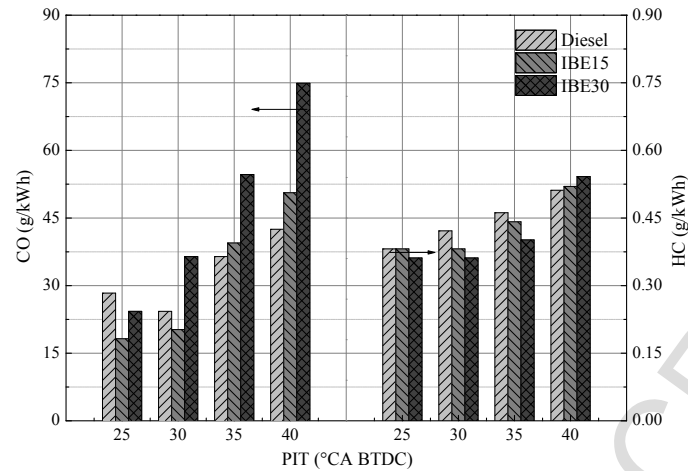


346  
 347 **Fig. 9.** BTE and BSFC for different fuels with various PITs.

### 348 3.2.3. Emission characteristics

349 The variation of the CO and HC emissions with different PITs for the different fuels are  
 350 given in Fig. 10. The results show that when the PIT is advanced, the CO and HC emissions for  
 351 the double injection are first lowered and then increased in comparison to the single injection  
 352 conditions. In general, the evaporation or combustion of the pilot fuel can promote the  
 353 combustion of the main injection fuel and thus cause the CO and HC emissions to reduce.  
 354 Nevertheless, when the PIT is over advanced, the pilot fuels are hard to auto-ignite and undergo a  
 355 poor evaporation process, which may have a negative effect on the main injection. In addition,  
 356 the over advanced PIT postpones the combustion phasing significantly, thus more unburned fuels  
 357 are trapped in crevices and deposits escape to exhaust emissions directly. It also shows that a  
 358 small PIT is helpful for IBE15 and IBE30 to reduce CO and HC emissions. Compared with pure  
 359 diesel, CO and HC emissions for the two fuel blends are lower at small PIT. However, when the  
 360 PIT is advanced, the CO and HC emissions for IBE15 and IBE30 increase rapidly. Eventually,

361 the CO and HC emissions for IBE15 and IBE30 are higher than that of pure diesel.



362

363 **Fig. 10.** CO and HC emissions for different fuels with various PITs.

364 The changes of NO<sub>x</sub> and soot emissions along with PITs for different fuels are presented in  
 365 [Fig. 11](#). Compared to the previous case with no pilot injection, it can be clearly seen that the  
 366 addition of a pilot injection can reduce NO<sub>x</sub> emissions by almost a quarter at the same power  
 367 output. This is mainly because the pilot injection helps to shorten the ignition delay, and then  
 368 contributes to the improvement of the diffusion combustion and weakens the premixed  
 369 combustion. However, the soot emissions for the double injection increase in comparison with  
 370 the single injection condition. This is also due to the improved diffusion combustion.  
 371 Additionally, it can be found that when PIT is advanced, NO<sub>x</sub> emissions for all the tested fuels  
 372 slightly increase since the premixed combustion is enhanced by the prolongation of ignition delay  
 373 and the enhancement of premixed combustion. On the contrary, soot emissions decrease for all  
 374 the tested fuels as the PIT is advanced due to the same reason. Compared with pure diesel, both  
 375 IBE15 and IBE30 also present a promising potential to reduce soot emissions under the  
 376 conditions of double injection.

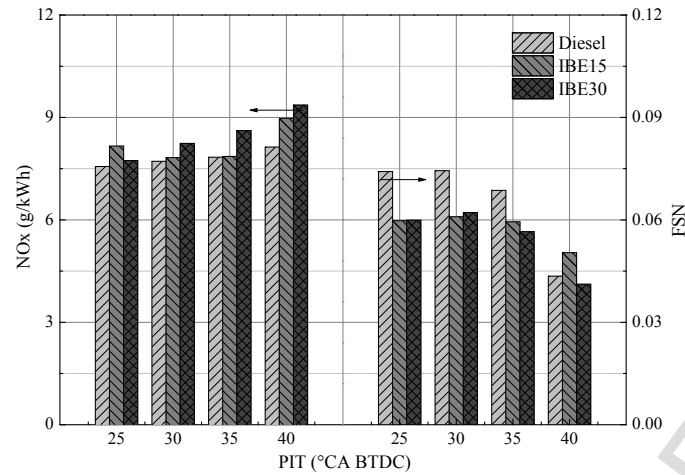


**Fig. 11.** NO<sub>x</sub> and soot emissions for different fuels with various PITs.

377

378

### 379 3.3. Visualization of combustion process

380

381

382

383

384

385

386

387

388

389

390

391

392

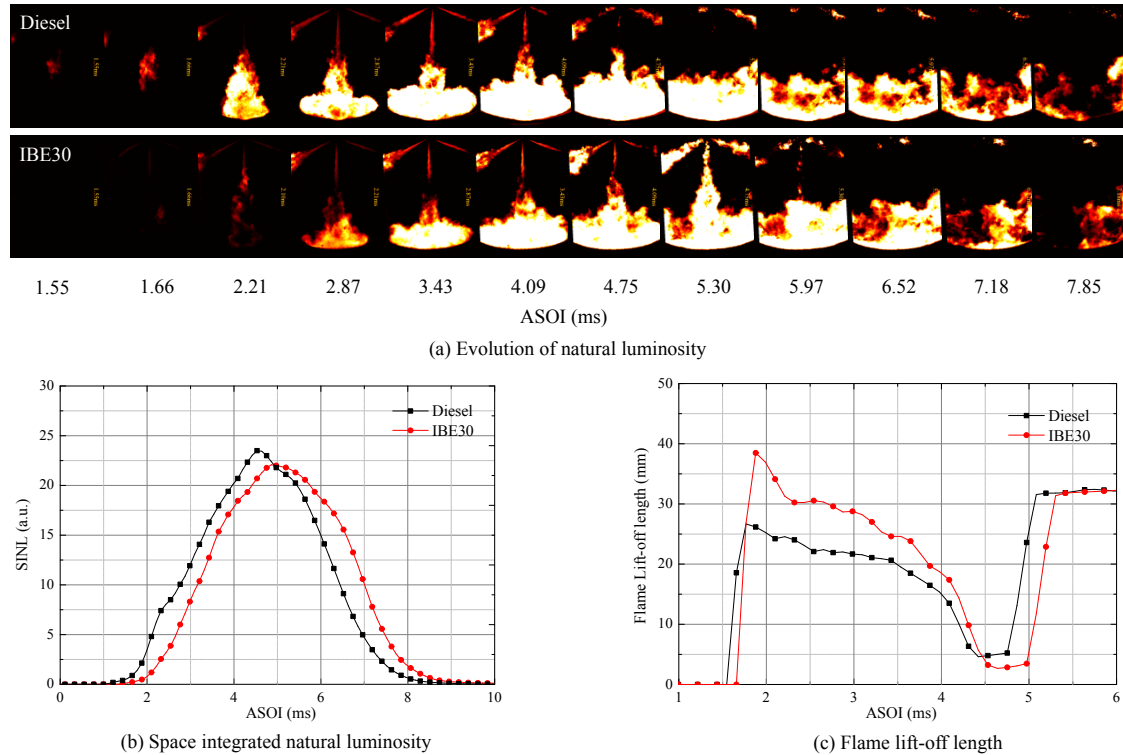
393

In order to further study the combustion process of the IBE and diesel blends, detailed experiments were conducted on a premixed combustion heated constant volume chamber. The detailed specifications of the chamber and the schematic of the chamber setup are given in [17-19]. The difference is that the injector used in current work was uninstalled from the AVL diesel engine. It had six holes and the orifice diameter measured by a microscopic was 0.15 mm. During the experiments, the injection duration and pressure were maintained for 3 ms and 60 MPa, respectively. Furthermore, the ambient density of the chamber was kept at 15 kg/m<sup>3</sup> and the ambient temperature at the time where the fuel injected was kept at 1000 K. Moreover, the experiments were conducted under a normal oxygen concentration, namely 21%, to simulate the engine combustion without EGR.

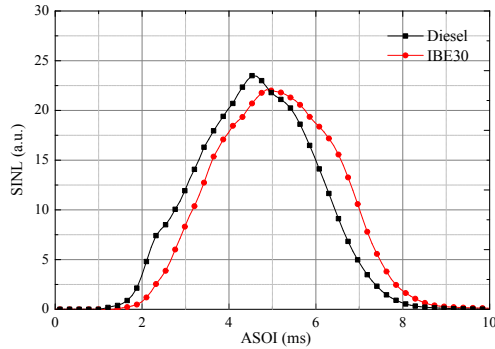
The combustion process of the pure diesel and IBE30 in the constant volume chamber are displayed in Fig. 12. Fig. 12(a) shows the natural flame evolution of pure diesel and IBE30. The original gray images have been converted to pseudo-color images in MATLAB for a better display effect. The colors in the images only represent an arbitrary unit scale consistent over the

394 whole combustion process. The images presented in a single row are sequences from one  
395 individual injection. In each image, the center of the top edge is the injector tip while the other  
396 edge is the curved wall. It can be found that compared with pure diesel, the intensity of the flame  
397 luminosity of the fuel blends is much lower. Since the natural luminosity is mainly contributed by  
398 the soot incandescence, it is reasonable to say this result is a strong support of the FSN results  
399 recorded from diesel engine. The ignition delay or illumination delay can be identified as the  
400 interval between the injection timing and the start point of the flame luminosity. It can be seen  
401 that the IBE30 has a longer ignition delay over pure diesel. That is also exactly the same result as  
402 diesel engine.

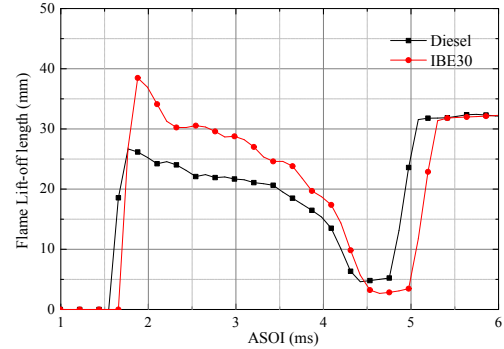
403 [Fig. 12 \(b\)](#) gives the changes of the space integrated natural luminosity (SINL). The SINL  
404 was calculated by summing up the values of all pixel in the entire luminosity image and averaged  
405 over five different runs at the same experimental conditions. It is shown that the SINL of IBE30  
406 is lower than that of pure diesel. This is mainly due to the lower soot emissions of IBE30. The  
407 flame lift-off length for both pure diesel and IBE30 are given in [Fig. 12 \(c\)](#). The flame lift-off  
408 length is defined as the interval between the injector tip and the point where significant flame  
409 luminosity is captured. The results shown that the flame lift-off length of IBE30 is longer than  
410 that of pure diesel because that the flame lift-off length is mainly controlled by the ignition delay,  
411 and a longer ignition delay usually results in a longer flame lift-off length. In general, the fuel  
412 undergoes more time to mixing at long flame lift-off length, hence the equivalence ratio at the  
413 flame zone can be effectively reduced. This can be used to explain the results why soot emissions  
414 of IBE30 are lower than that of pure diesel.



(a) Evolution of natural luminosity



(b) Space integrated natural luminosity



(c) Flame lift-off length

415

416 **Fig. 12.** Combustion process of pure diesel and IBE30 in a constant volume chamber.

#### 417 4. Conclusions

418 A detailed experimental investigation was conducted on a single cylinder and common-rail  
 419 diesel engine fueled with IBE and diesel blends to evaluate the effects of injection strategies on  
 420 engine performance, combustion, and emissions. The conclusions are drawn as follows:

421 (1) In the single injection cases, the peak in-cylinder pressure and *HRR* increase significantly  
 422 for all the tested fuels and their peak values are gradually advanced as the MIT is advanced.  
 423 Compared with pure diesel, the peak in-cylinder pressure and *HRR* of IBE15 and IBE30 are  
 424 higher and their peak values appear later. Taking in consideration of the engine performance and  
 425 economy, the optimal MIT for the pure diesel and IBE15 is 12 °CA BTDC but for IBE30 is 9  
 426 °CA BTDC.

427 (2) Additionally, CO and HC emissions for all the tested fuels reduce when the MIT is  
 428 advanced from 6 to 15 °CA BTDC, but then increase when the MIT is further advanced. At

429 almost all test conditions, both IBE15 and IBE30 can effectively reduce soot emissions, but  
430 contribute to an increase in NO<sub>x</sub> emissions. Further optimization for soot emissions can be  
431 achieved by advancing the MIT, but the NO<sub>x</sub> emissions may increase in this case.

432 (3) When the pilot injection is adopted, the pressure and *HRR* curve for all the tested fuels  
433 become less severe and their peak values are lower in comparison to the single-injection  
434 condition. The *HRR* curve for diesel and IBE15 presents a double or triple peak profile at a small  
435 PIT while a single peak profile at large PIT. However, for IBE30, its *HRR* curve always presents  
436 a single peak profile. Furthermore, a pilot injection is helpful to improve both engine  
437 performance and economy for all the tested fuels, especially IBE30.

438 (4) A small PIT is helpful to reduce CO and HC emissions but a large PIT causes the CO  
439 and HC emissions to increase. Additionally, it is found that CO and HC emissions for the two  
440 fuel blends are lower than that of pure diesel at a small PIT. However, when the PIT is advanced,  
441 the CO and HC emissions for IBE15 and IBE30 increase rapidly, and eventually higher than that  
442 of pure diesel. A pilot injection is favorable to reduce NO<sub>x</sub> emissions, but results in higher soot  
443 emissions. Furthermore, as the PIT is advanced, the NO<sub>x</sub> emissions are slightly elevated but the  
444 soot emissions decrease significantly.

445 (5) Compared with pure diesel, the intensity of flame luminosity of the IBE30 is lower and  
446 the illumination delay is shorter. Moreover, the flame lift-off length of IBE30 is much longer than  
447 pure diesel. The longer flame lift-off length means the fuel undergoes more time to mixing,  
448 which causes the equivalence ratio at the flame zone to reduce. This feature may contribute to  
449 lean homogenous combustion and less soot emissions.

450 (6) From the results presented in this study. The optimum condition is IBE15 with main

451 injection timing of 9 °CA BTDC and pilot injection of 30 °CA BTDC. At this condition, the  
452 engine has high BTE but low BSFC. Furthermore, both NO<sub>x</sub> and soot emissions are kept in a low  
453 level.

#### 454 **Acknowledgement**

455 This study was finished in University of Illinois at Urbana-Champaign and supported by the  
456 National Science Foundation under Grant No. CBET-1236786. This work was also supported by  
457 the China Scholarship Council under Grant No. 201606560027.

#### 458 **References**

- 459 [1] B.S. Chauhan, R.K. Singh, H.M. Cho, H.C. Lim. Practice of diesel fuel blends using  
460 alternative fuels: A review. *Renewable Sustainable Energy Rev* 2016; 59:1358-1368.
- 461 [2] B.R. Kumar, S. Saravanan, D. Rana, A. Nagendran. Use of some advanced biofuels for  
462 overcoming smoke/NO<sub>x</sub> trade-off in a light-duty DI diesel engine. *Renewable Energy* 2016;  
463 96: 687-699.
- 464 [3] C. Cen, H. Wu, C.F. Lee, F. Liu, Y. Li. Experimental investigation on the characteristic of jet  
465 break-up for butanol droplet impacting onto a heated surface in the film boiling regime. *Int J*  
466 *Heat Mass Tran* 2018; 123:129-136.
- 467 [4] Z.H. Zhang, R. Balasubramanian. Influence of butanol–diesel blends on particulate emissions  
468 of a non-road diesel engine. *Fuel* 2014; 118:130-136.
- 469 [5] X.B. Cheng, S. Li, J. Yang, B. Liu. Investigation into partially premixed combustion fueled  
470 with N-butanol-diesel blends. *Renewable Energy* 2016; 86:723-732.
- 471 [6] H. Huang, Q. Liu, R. Yang, T. Zhu, R. Zhao, Y. Wang. Investigation on the Effects of pilot  
472 injection on low temperature combustion in high-Speed diesel engine fueled with n-butanol–

- 473 diesel blends. *Energy Convers Manage* 2015; 106:748-58.
- 474 [7] S.S. Merola, C. Tornatore, S.E. Iannuzzi, L. Marchitto, G. Valentino. Combustion process  
475 investigation in a high-speed diesel engine fueled with n-butanol diesel blend by conventional  
476 methods and optical diagnostics. *Renewable Energy* 2014, 64:225-237.
- 477 [8] Z. Chen, Z. Wu, J. Liu, C. Lee. Combustion and emissions characteristics of high n-  
478 butanol/diesel ratio blend in a heavy-duty diesel engine and EGR impact. *Energy Convers*  
479 *Manage* 2014; 78:787-95.
- 480 [9] N. Qureshi, T.C. Ezeji. Butanol, 'a superior biofuel' production from agricultural residues  
481 (renewable biomass): recent progress in technology. *Biofuel Bioprod Biorefin* 2008; 2:319-  
482 30.
- 483 [10] K. Kraemer, A. Harwardt, R. Bronneberg, W. Marquardt. Separation of butanol from  
484 acetone-butanol-ethanol fermentation by a hybrid extraction-distillation process. *Comput*  
485 *Chem Eng* 2011; 35:949-63.
- 486 [11] A.S. Afschar, H. Biebl, K. Schaller, K. Schugerl. Production of acetone and butanol by  
487 *clostridium-acetobutylicum* in continuous culture with cell recycle. *Appl Microbiol Biot*  
488 1985; 22:394-8.
- 489 [12] M. Kumar, Y. Goyal, A. Sarkar, K. Gayen. Comparative economic assessment of ABE  
490 fermentation based on cellulosic and non-cellulosic feedstocks. *Appl Energy* 2012; 93:93-  
491 204.
- 492 [13] Y.Q. Li, K. Nithyanandan, T.H. Lee, R.M. Donahue, Y.L. Lin, C.F. Lee. Effect of water-  
493 containing acetone-butanol-ethanol gasoline blends on combustion, performance, and  
494 emissions characteristics of a spark-ignition engine. *Energy Convers Manage* 2016; 117:21-

495 30.

- 496 [14] K. Nithyanandan, J. Zhang, Y. Li, H. Wu, T.H. Lee, Y. Lin. Improved SI engine efficiency  
497 using acetone–butanol–ethanol (ABE). *Fuel* 2016; 174:333-43.
- 498 [15] T. Lee, Y. Lin, X. Meng, Y. Li. Combustion characteristics of acetone, butanol, and ethanol  
499 (ABE) blended with diesel in a compression-ignition engine. *SAE Technical Paper* 2016;  
500 2016-01-0884.
- 501 [16] Y. Lin, T. Lee, K. Nithyanandan, J. Zhang. Experimental investigation and analysis of  
502 combustion process in a diesel engine fueled with acetone-butanol-ethanol/ diesel blends.  
503 *SAE Technical Paper* 2016; 2016-01-0737.
- 504 [17] H. Wu, K. Nithyanandan, J.X. Zhang, Y.L. Lin, T.H. Lee, C.F. Lee. Impacts of acetone-  
505 butanol-ethanol (ABE) ratio on spray and combustion characteristics of ABE-diesel blends.  
506 *Appl Energy* 2015; 149:367-78.
- 507 [18] H. Wu, K. Nithyanandan, N. Zhou, T.H. Lee, C.F. Lee, C.H. Zhang. Impacts of acetone on  
508 the spray combustion of acetone-butanol-ethanol (ABE)-diesel blends under low ambient  
509 temperature. *Fuel* 2015; 142:109-16.
- 510 [19] H. Wu, T.H. Lee, C.F. Lee, F. Liu, B. Sun. Optical soot measurement of bio-butanol  
511 upstream product, ABE (acetone–butanol–ethanol), under diesel-like conditions. *Fuel* 2016;  
512 181:300-9.
- 513 [20] N. Zhou, M. Huo, H. Wu, K. Nithyanandan, C.F. Lee, Q.N. Wang. Low temperature spray  
514 combustion of acetone-butanol-ethanol (ABE) and diesel blends. *Appl Energy* 2014;  
515 117:104-15.
- 516 [21] K. Han, B. Pang, X. Ma, H. Chen, G. Song, Z. Ni. An experimental study of the burning

- 517 characteristics of acetone–butanol–ethanol and diesel blend droplets. *Energy* 2017; 139:853-  
518 61.
- 519 [22] X. Ma, F. Zhang, K. Han, B. Yang, G. Song. Evaporation characteristics of acetone–  
520 butanol–ethanol and diesel blends droplets at high ambient temperatures. *Fuel* 2015; 160:43-  
521 9.
- 522 [23] J.Y. Lee, Y.S. Jang, J. Lee, E.T. Papoutsakis, S.Y. Lee. Metabolic engineering of  
523 *Clostridium acetobutylicum* M5 for highly selective butanol production. *Biotechnol J.* 2009;  
524 4:1432–1440.
- 525 [24] S.B. Tummala, N.E. Welker, E.T. Papoutsakis. Design of antisense RNA constructs for  
526 downregulation of the acetone formation pathway of *Clostridium acetobutylicum*. *J Bacteriol.*  
527 2003; 185:1923–1934.
- 528 [25] Y. Jiang, C. Xu, F. Dong, Y. Yang, W. Jiang, S. Yang. Disruption of the acetoacetate  
529 decarboxylase gene in solvent-producing *Clostridium acetobutylicum* increases the butanol  
530 ratio. *Metab Eng.* 2009; 11:284–291.
- 531 [26] S. Dusséaux, C. Croux, P. Soucaille, I. Meynial-Salles. Metabolic engineering of *clostridium*  
532 *acetobutylicum* ATCC 824 for the high-yield production of a biofuel composed of an iso-  
533 propanol/butanol/ethanol mixture. *Metabolic Eng* 2013; 18:1-8.
- 534 [27] S.B. Bankar, G. Jurgens, S.A. Survase, H. Ojamo, T. Granstrom. Enhanced iso-propanol-  
535 butanol-ethanol (IBE) production in immobilized column reactor using modified *clostridium*  
536 *acetobutylicum* DSM792. *Fuel* 2014; 136:226-32.
- 537 [28] Y.S. Jang, A. Malaviya, J. Lee, J.A. Im, S.Y. Lee, J. Lee. Metabolic engineering of  
538 *clostridium acetobutylicum* for the enhanced production of iso-propanol-butanol-ethanol fuel

- 539 mixture. *Biotechnol Prog* 2013; 29:1083-8.
- 540 [29] Y.Q. Li, L. Meng, K. Nithyanandan, T.H. Lee, Y.L. Lin, C.F. Lee. Combustion,  
541 performance and emissions characteristics of a spark-Ignition engine fueled with iso-  
542 propanol-n-butanol-ethanol and gasoline blends. *Fuel* 2016; 184:864-72.
- 543 [30] Y.Q. Li, Y. Chen, G. Wu, C.F. Lee, J.W. Liu. Experimental comparison of acetone-n-  
544 butanol-ethanol (ABE) and isopropanol-n-butanol-ethanol (IBE) as fuel candidate in spark-  
545 ignition engine. *Appl Therm Eng* 2018; 133:179-187.
- 546 [31] T. Lee, H. Wu, A. Hansen, T. Lee. Comparison study on combustion and emission  
547 characteristics of ABE/IBE-diesel blends in a common-rail diesel engine. *SAE Technical*  
548 *Paper* 2017; 2017-01-2321.
- 549 [32] G. Li, Z.E. Liu, T.H. Lee, C.F. Lee, C.H. Zhang. Effects of dilute gas on combustion and  
550 emission characteristics of a common-rail diesel engine fueled with isopropanol-butanol-  
551 ethanol and diesel blends, *Energy Convers Manage* 2018; 165:373-381.
- 552 [33] M. Lapuerta, J. Rodríguez-Fernández, D. Fernández-Rodríguez, R. Patiño-Camino.  
553 Modeling viscosity of butanol and ethanol blends with diesel and biodiesel fuels. *Fuel* 2017;  
554 199: 332-338.
- 555 [34] K. Nithyanandan, J. Zhang, Y.Q. Li, H. Wu. Investigating the impact of acetone on the  
556 performance and emissions of acetone-butanol-ethanol (ABE) and gasoline blends in an SI  
557 engine. *SAE Technical Paper* 2015; 2015-01-0909.
- 558 [35] A.O. Emiroğlu, M. Şen. Combustion, performance and exhaust emission characterizations of  
559 a diesel engine operating with a ternary blend (alcohol-biodiesel-diesel fuel). *Appl Therm*  
560 *Eng* 2018; 133:371-380.

- 561 [36] C. Özer, E. Öztürk, H.S. Yücesu. Combustion and exhaust emissions of canola biodiesel  
562 blends in a single cylinder DI diesel engine. *Renewable Energy* 2017; 109:73-82.
- 563 [37] J. Hwang, D.H. Qi, Y.J. Jung, C. Bae. Effect of injection parameters on the combustion and  
564 emission characteristics in a common-rail direct injection diesel engine fueled with waste  
565 cooking oil biodiesel. *Renewable Energy* 2014; 63:9-17.
- 566 [38] Z. Şahin, O.N. Aksu. Experimental investigation of the effects of using low ratio n-  
567 butanol/diesel fuel blends on engine performance and exhaust emissions in a turbocharged DI  
568 diesel engine. *Renewable Energy* 2015; 77:279-290.
- 569 [39] J.F. Luo, Y.M. Zhang, J.J. Wang, Q.X. Zhang. Effect of acetone–butanol–ethanol addition to  
570 diesel on the soot reactivity. *Fuel* 2018; 226:555-563.
- 571 [40] A. Maghbouli, W.M. Yang, H. An, J. Li, S. Shafee. Effects of injection strategies and fuel  
572 injector configuration on combustion and emission characteristics of a D.I. diesel engine  
573 fueled by bio-diesel. *Renewable Energy* 2015; 76:687-698.

#### 574 **Abbreviation**

575	ABE	acetone-butanol-ethanol
576	BMEP	brake mean effective pressure
577	BSFC	brake specific fuel consumption
578	BTDC	before top dead center
579	BTE	brake thermal efficiency
580	CA	crank angle
581	EOC	end of combustion
582	FSN	filter smoke number

583	HC	hydrocarbons
584	<i>HRR</i>	heat release rate
585	IBE	isopropanol-butanol-ethanol
586	MIT	main injection timing
587	NO <sub>x</sub>	nitrogen oxide
588	PB	paper blackening
589	PIT	pilot injection timing
590	SI	spark ignition
591	SINL	space integrated natural luminosity
592	SOC	start of combustion
593	TDC	top dead center
594	$T_{inj}$	temperature at the crank angle where the fuel injected

**Highlights**

Characters of IBE and diesel blends at different injection strategies were studied.

Injection strategy affects the combustion process of IBE and diesel blends greatly.

Maximum pressure and HRR are obviously reduced when adopting a pilot injection.

Both engine performance and economy are improved under double injection conditions.

Double injection is helpful to reduce NO<sub>x</sub> emissions while increase soot emissions.